Comparative analysis of empirical parametrization and microscopical studies of deuteron-induced reactions

M. Avrigeanu and V. Avrigeanu
Horia Hulubei National Institute for Physics and Nuclear Engineering, P.O. Box MG-6, 077125 Bucharest-Magurele, Romania

Abstract
An extended analysis of the deuteron–induced reactions is carried out paying due consideration to both the reaction cross-section parametrization procedure and theoretical models associated to the deuteron interaction process. The key role of direct interactions, i.e., breakup, stripping and pick-up processes is stressed out by the comparison of data with theoretical and evaluation predictions.

1 Introduction

So far the Hauser-Feshbach statistical model has mainly been involved as the main tool to calculate the deuteron reaction cross sections at low and medium incident energies, the compound-nucleus (CN) mechanism being considered to be dominant within this energy range. However, the specific non-compound processes direct interactions (DI), namely breakup, stripping and pick-up, make substantially different the deuteron-induced reactions than the case of other incident particles. Therefore, neglected peculiarity of the deuteron interaction process is evidenced by the apparent discrepancies between the data and either theoretical or evaluated predictions. The specific reaction mechanism among the deuteron DI is the breakup (BU), particularly important due to the large variety of reactions initiated by the breakup nucleons along the whole incident-energy range [1]. Moreover, the role of the deuteron BU increases with the target-nucleus mass and charge, so that it becomes dominant for heavy target nuclei at deuteron incident energies particularly around the Coulomb barrier [2]. Otherwise, the deuteron interaction with low- and medium-mass target nuclei below and around the Coulomb barrier proceeds largely through stripping and pick-up direct reactions (DR) mechanisms, while pre-equilibrium emission (PE) and evaporation from fully equilibrated CN become important at higher energies [1, 3–5].

However, while the associated models for DR, PE, and CN mechanisms are already settled, an increased attention should be paid to the theoretical description of the BU-mechanism two components, namely the elastic breakup (EB), with no interaction target nucleus–breakup nucleons, and inelastic BU or breakup fusion (BF), where one of these constituents interacts non-elastically with the target nucleus. This is why a comparative assessment of measured data and results of BU microscopic description [6, 7] as well as current parametrization [9] already involved within recent systematic studies [1–5] are equally useful to basic studies and improved nuclear data evaluations.

Obviously an update of the theoretical analysis of deuteron-nuclei interaction within a consistent account of the related reaction mechanisms is highly requested not only by the strategic research programs as the International Thermonuclear Experimental Reactor (ITER) [10], the International Fusion Material Irradiation Facility (IFMIF) [11], in connection with the ITER program, and the Neutron For Science (NFS) project at SPIRAL-2 facility [12], but also by use of deuteron surrogate reactions for (n, γ) and (n, f) cross sections [2], of interest for breeder reactors studies, as well as by medical investigations using accelerated deuterons [13].

2 reaction cross-section parametrization vs model analysis

The reaction cross-section parametrization within the analysis of the most important deuteron induced reactions, the deuteron monitor reactions, has been recommended by Hermanne *et al.* [13] in a recent

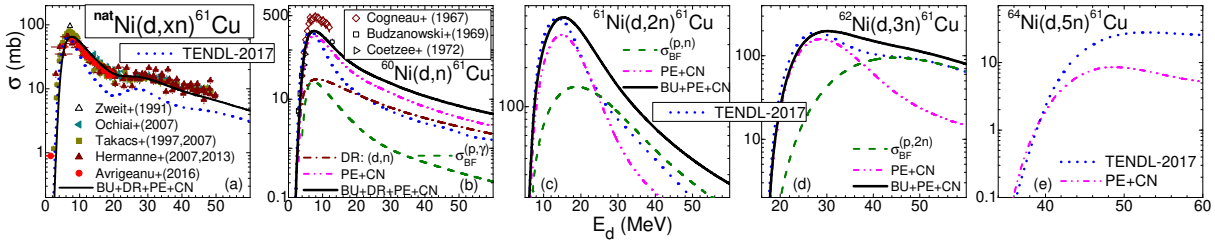

Fig. 1: (Color online) Comparison of measurements [14], TENDL-2017 [15] evaluation (dotted curves), and model calculation (solid curves) of ^{nat}Ni$(d,xn)^{61}$Cu, ^{60}Ni$(d,n)^{61}$Cu, ^{61}Ni$(d,2n)^{61}$Cu, ^{62}Ni$(d,3n)^{61}$Cu, and ^{64}Ni$(d,5n)^{61}$Cu reaction cross sections, along with BF enhancement (dashed curves), stripping (d,n) reaction (dash-dotted curve), and PE+CN components (dash-dot-dotted curves) corrected for DI deuteron flux leakage [4].

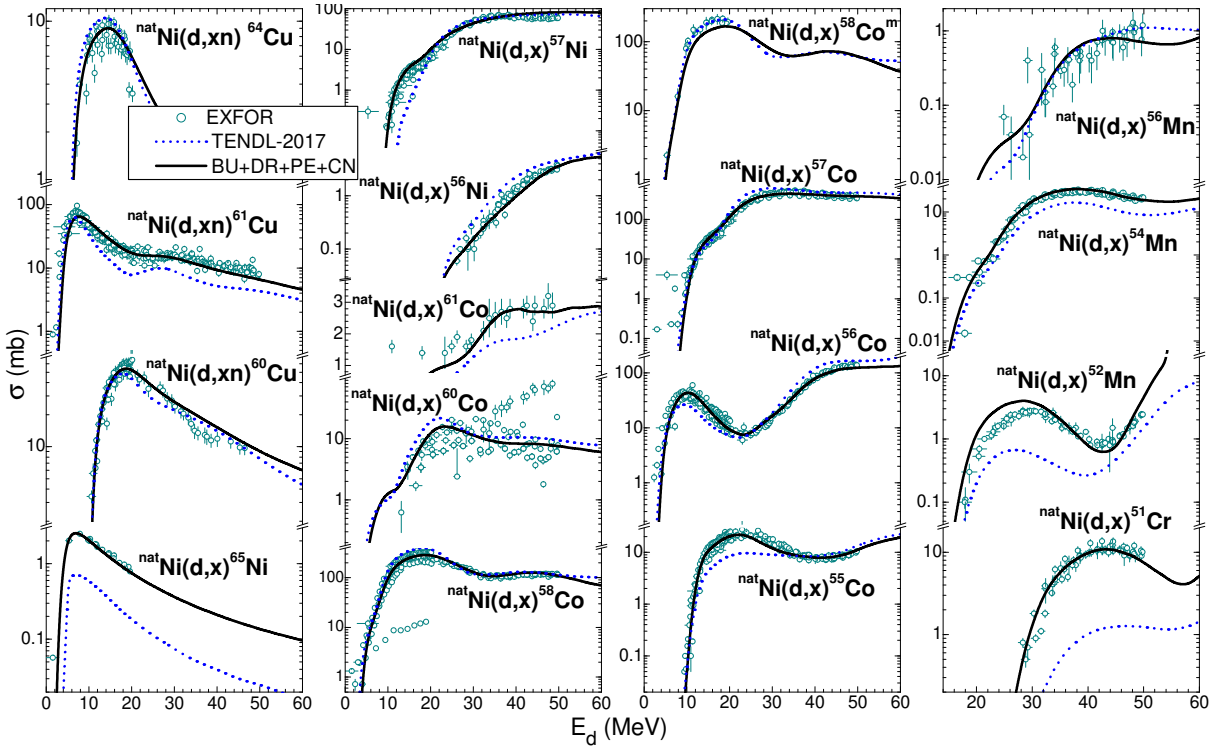

Fig. 2: Comparison of measurements (solid circles) [14], TENDL-2017 [15] evaluation (short-dotted curves), and model calculations (solid curves) of excitation functions for deuteron-induced reactions on ^{nat}Ni [4].

paper published in a Special Issue on Nuclear Reaction Data. Thus, for the comparative analysis of both experimental data and theoretical predictions and the final evaluation, the authors replaced the theory by Padé fit, with so low predictive power and apart from nuclear modeling advance.

A consistent and unitary nuclear reaction mechanisms analysis, considering all contributing Ni isotopes, is interposed to their Padé fit of the experimental ^{nat}Ni$(d,xn)^{61}$Cu excitation function (Fig. 20 (b) of Ref. [13]). The corresponding results are shown in Fig. 1 [4] including also the TENDL-2017 evaluation predictions [15]. The most complete picture of the involved mechanisms for the population of ^{61}Cu residual nucleus is shown in Fig. 1(b). The consequent model calculations including the contributions from the breakup process through the (p,γ) reaction initiated by breakup protons, the (d,n) stripping reaction, as well as statistical pre-equilibrium and compound nucleus mechanisms, describe the experimental ^{60}Ni$(d,n)^{61}$Cu excitation function [14], except the oldest Cogneau *et al.* data [14], totally discrepant with those reported for natural Ni target too. Important contribution to the population

of ^{61}Cu residual nucleus comes also from ^{61}Ni$(d,2n)$ and ^{62}Ni$(d,3n)$ processes, Fig. 1(c,d), where the competition between the deuteron-induced PE+CN and the inelastic breakup through ^{61}Ni(p,n) and respectively ^{62}Ni$(p,2n)$ processes changes toward breakup mechanism for the incident energies of $\sim$ 25 MeV and 35 MeV, respectively. Thus, the breakup contributions make slower the decrease of the (d,xn) excitation function, comparing with their steep increase above the threshold. The disregard of the breakup and the stripping mechanisms contributions leads to the underestimation of both ^{nat}Ni$(d,x)^{61}$Cu [14] and ^{60}Ni$(d,n)^{61}$Cu [14] experimental excitation functions, e.g., TENDL–2017 evaluations (dotted curves), [15] shown in Fig. 1(a,b).

Actually almost all deuteron-induced monitor reactions described with Padé fit by Hermanne *et al.* [13] have already been analyzed in the frame of breakup, stripping, pick-up, pre-equilibrium emission and compound nucleus reaction mechanisms models [3–5]. These analyzes covered the whole experimental systematics of the deuteron induced reactions on the natural element of interest, e.g., updated Fig. 2 from Ref. [4] by considering the TENDL-2017 evaluation predictions [15]. There are included among them the specific monitor reactions ^{nat}Ni$(d,x)^{56}$Co, ^{nat}Ni$(d,x)^{58}$Co, and ^{nat}Ni$(d,xn)^{61}$Cu. Moreover, as long as there exist both available dedicated codes for nuclear reactions calculations and the powerful computers, the complexity of deuteron interactions can not motivate the use of Padé approximations [13] for the analysis of measured deuteron–reaction cross sections.

3 Breakup

Our analyzes of the deuteron breakup mechanism are based on the parametrization [8, 9] of both the total breakup (EB+BF) and EB data, assuming that the inelastic-breakup cross section for neutron emission σ^{n}_{BF} is the same as that for the proton emission σ^{p}_{BF} (e.g., Ref. [16]), so that the total breakup cross sections σ_{BU} is given by the sum σ_{EB}+2$\sigma^{n/p}_{BF}$. The parametrization has concerned the total BU nucleon-emission and EB fractions, i.e. $f^{n/p}_{BU} = \sigma^{n/p}_{BU}/\sigma_R$ and f_{EB}=σ_{EB}/σ_R, respectively, where σ_R is the deuteron total-reaction cross section. The dependence of these fractions on the deuteron incident energy E and the target-nucleus atomic Z and mass A numbers was obtained [9] through analysis of the experimental systematics of deuteron-induced reactions on target nuclei from ^{27}Al to ^{232}Th and incident energies up to 80 MeV for the former [17], but within a more restricted energy range up to 30 MeV [16, 17] for the latter. Because of that, the correctness of the extrapolation of elastic breakup parametrization has been checked [18] by comparison with results of the microscopic continuum-discretized coupled-channels (CDCC) method [19]. Thus, a normalization factor has been introduced for the extrapolation of f_{EB} at energies beyond the available data, in agreement with the behavior of f^{p}_{BU} and the CDCC calculation results [9]. Nevertheless, the empirical parametrization should be confirmed by further data measurements and also advanced theoretical modeling.

The comparison of the measured total BU proton-emission cross sections σ^{p}_{BU} at 15, 25.5, 56, 70 and 80 MeV deuteron energies and for target nuclei from ^{12}C to ^{232}Th [17], with the above-described parametrization and the microscopic cross sections obtained in the frame of the CDCC extension of the eikonal reaction theory (ERT), using microscopic optical potentials by Neoh *et al.* [6] and those of Carlson *et al.* [7] obtained in the frame of distorted wave Born approximation (DWBA) method with post form interaction and zero–range approach is shown in Fig. 3 (a-d). Since the absolute cross sections may depend on the model ingredients of reaction mechanisms involved within the experimental data analysis, e.g., optical-potential and PE model parameters, a similar comparative analysis concerns at the same time in Fig. 3 (e-h) the corresponding total BU proton-emission fractions f^{p}_{BU}. On the other hand, the f^{p}_{BU} values may illustrate the importance of the breakup process among the other reaction mechanisms related to the deuteron interactions. Moreover, the same scale has been used for σ^{p}_{BU} as well as f^{p}_{BU} values at all incident energies of the available experimental data, in order to make also possible an assessment of their energy dependence.

There are several features which are pointed out by this comparative analysis. First, the increase

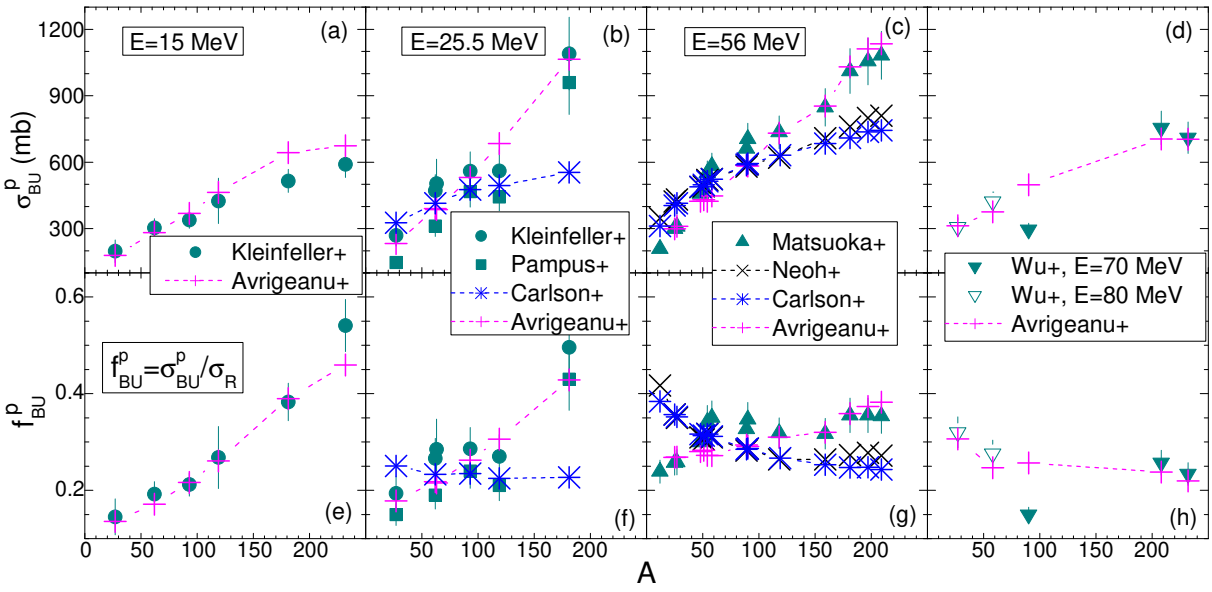

Fig. 3: (Color online) Comparison of the mass dependence of measured (solid circle, ■, ▲, ▼, ▽) [17] total BU proton-emission cross sections (top) and fractions (bottom) with the predictions of the microscopic eikonal model [6] (×), DWBA formalism [7] (∗), and of the empirical parametrization (+), connected by dashed lines for eye guiding, for target nuclei from ^{12}C up to ^{209}Bi, at the incident energies of 15, 25.5, 56, 70, and 80 MeV.

of σ^p_{BU} with the target-nucleus mass is well described by the empirical parametrization for all deuteron energies from 15 to 80 MeV. There is a similar trend of the microscopic results for medium-mass nuclei with $40<A<120$, while it is apparent an overestimation of the measured data for light nuclei ($A<40$) at both 25 and 56 MeV incident energies, as well as an underestimation for heavier ones ($A>120$). Second, the importance of the BU mechanism, shown by f^p_{BU}, is increasing with the target-nucleus mass, from ^{27}Al up to ^{232}Th, at the lower incident energies of 15 and 25.5 MeV. This increase is less significant at the energy of 56 MeV, and even reversed at 70-80 MeV. Actually it seems that the fraction f^p_{BU} has reached its maximum at 56 MeV, for the target nuclei with $A>120$, while for $40<A<120$ this maximum moves at energies over 56 MeV but lower than 70-80 MeV. Moreover, the f^p_{BU} values are still increasing with the incident energy even at 80 MeV for the deuteron interaction with light target nuclei ($A<40$). These energy dependencies of the measured f^p_{BU} are satisfactorily described by the empirical parametrization. The microscopic results at 25 MeV [7] show almost constant f^p_{BU} for the whole A interval analyzed, while at 56 MeV [6, 7] show a steep decrease for target nuclei from A=12 up to $A\sim120$, apart from the data, while for $A>120$ their underestimated values describe however the target-nucleus mass dependence.

Overall, there are actually two opposite effects of the deuteron breakup on the deuteron activation cross sections that should be considered. Firstly, the total-reaction cross section, that is shared among different outgoing channels, is reduced by the value of the total breakup cross section σ_{BU}. On the other hand, the BF component brings contributions to different reaction channels [1–5]. Thus, the absorbed proton or neutron following the deuteron breakup contributes to the enhancement of the corresponding (d, xn) or (d, xp) reaction cross sections, respectively. The compound nuclei in reactions induced by the BF nucleons differ by one unit of the atomic mass and maybe of also the atomic number than in deuteron-induced reactions, the partition of the BF cross section among various residual-nuclei population being triggered by the energy spectra of the breakup nucleons and the excitation functions of the reactions induced by these nucleons on the target nuclei [1–5]. In order to calculate the BF enhancement of, e.g., the (d, xn) reaction cross sections, the BF proton-emission cross section σ^p_{BF} should be (i) multiplied by the ratios $\sigma_{(p,x)}/\sigma^p_R$, corresponding to the enhancing reaction, (ii) convoluted with the Gaussian line shape

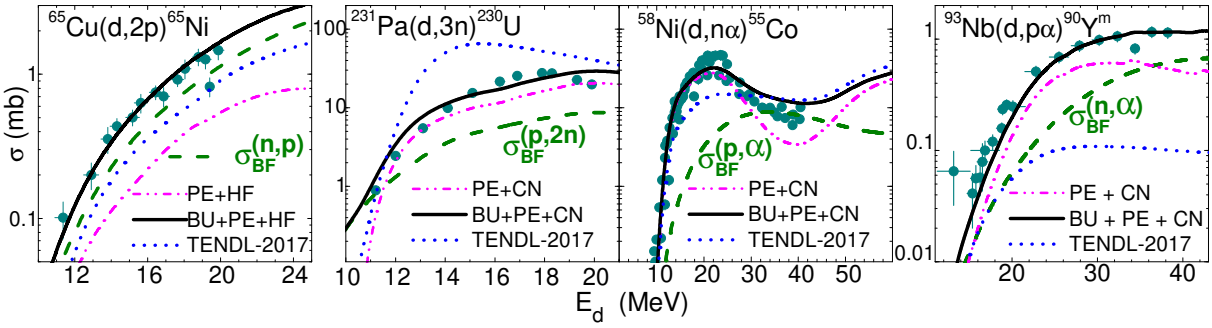

Fig. 4: (Color online) Comparison of measured deuteron activation cross sections [14], complete analysis results (thick solid curves) [2–4] taking into account the BF enhancement (dashed curves) and PE+CN contributions (dash-dot-dotted curves), and the TENDL-2017 evaluations (dotted curves) [15].

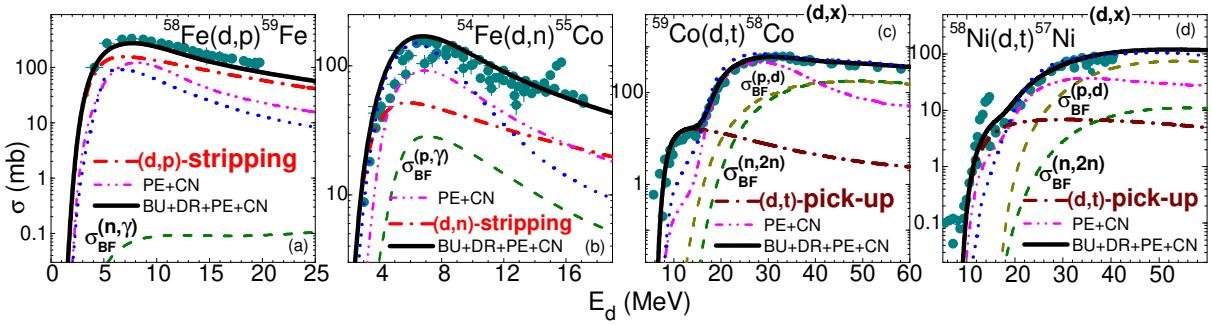

Fig. 5: (Color online) Comparison of measured deuteron activation cross sections [14], the TENDL-2017 evaluations (dotted curves) [15], and the analysis results (thick solid curves) [3,4] taking into account the BF enhancement (dashed curves), DR (dot-dashed curves), and PE+CN contributions (dash-dot-dotted curves).

distribution of the BF–proton energy E_p for a given deuteron incident energy E_d, and (iii) integrated over the BF proton energy. Consequently, the BF–enhancement cross section has the form [4]:

$$\sigma^{p,x}_{BF}(E_d) = \sigma^{p}_{BF}(E_d) \int_0^{E_d - B_d} dE_p \ \frac{\sigma_{(p,x)}(E_p)}{\sigma^{p}_{R}(E_p)} \frac{1}{(2\pi)^{\frac{1}{2}} w} exp[-\frac{(E_p - E^0_p)^2}{2w^2}] \ , \qquad (1)$$

where B_d is the deuteron binding energy, σ^p_R is the proton total reaction cross section, x stands for various γ, n, d, or α outgoing channels, while the Gaussian distribution parameters w and E^0_p are given by Kalbach [20].

The BF enhancements brought by the breakup neutron and proton interactions with various target nuclei from ^{54}Fe up to ^{231}Pa shown by dashed curves in Figs. 4 and 5 are important mainly for describing the excitation functions for second and third chance emitted-particle channels [2–4].

4 Direct reactions

The assessment of transfer reaction cross sections in addition to that of BU mechanism is mandatory for the final correct estimation of even the PE+CN contribution to population of various residual nuclei, in spite of poor attention given so far in deuteron activation analysis. However, a suitable estimation of DR cross sections is subject of available experimental spectroscopic factors, outgoing particle angular distributions, or at least the differential cross-section maximum values. The calculation of DR cross sections has been performed using the DWBA formalism within the FRESCO code [21]. The post/prior form distorted-wave transition amplitudes for the stripping and pick-up reactions, respectively, and the finite-range interaction have been considered. The n-p effective interaction in deuteron [22] as well as

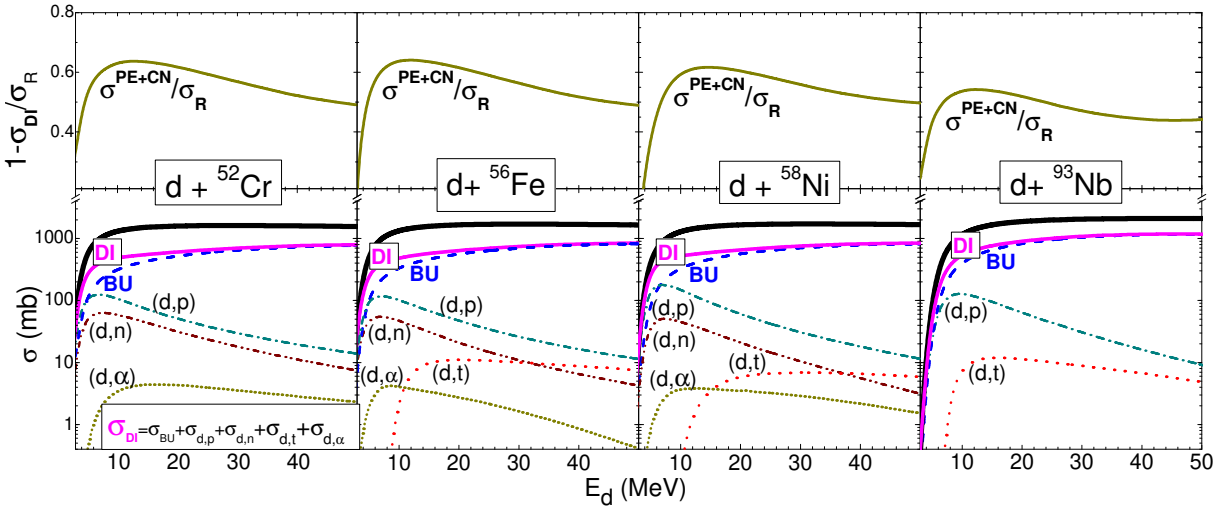

Fig. 6: (Color online) (Bottom) Total-reaction (solid curves), BU (dashed curves), stripping (d, n) (dash-dot-dotted curves) and (d, p) (dash-dotted curves), and pick-up (d, t) (dotted curves) and (d, α) (short-dotted curves) reaction cross sections for deuterons on ^{52}Cr, ^{56}Fe, ^{58}Ni, and ^{93}Nb [3–5]; (Top) the corresponding reduction factors of the deuteron flux going towards statistical processes (solid curves).

d-n effective interaction in triton [23] were assumed to have a Gaussian shape, at the same time with a Woods-Saxon shape [24] of the d-d effective interaction within the α particle. The transferred nucleon and deuteron bound states were generated in a Woods-Saxon real potential [3–5, 8]. The populated discrete levels and the corresponding spectroscopic factors which have been available within the ENSDF library [25] were used as the starting input for the DWBA calculations.

The significant effects of the stripping (d, p), (d, n), and pick-up (d, t) reactions for the deuteron interaction with ^{58}Fe, ^{54}Fe, and respectively with ^{59}Co and ^{58}Ni target nuclei have been reassessed in Fig. 5. It is thus proved that the direct reactions are quite important for the first-chance particle emission, the (d, p) stripping mechanism being the dominant mechanism for the (d,p) reactions [3–5], as can be seen from Fig. 5 (a). A particular note should also concern the pick–up essential contribution to the total (d, t) activation cross section at the energies between its threshold and those for the (d, nd) and $(d, 2np)$ reactions that lead to the same residual nucleus, see Fig. 5 (c,d).

Finally, we have taken into account the deuteron total-reaction cross section that remains available for the PE+CN mechanisms, following the correction for the incident flux leakage through direct interactions of the breakup, stripping and pick-up processes, given by a reduction factor:

$$1 - \frac{\sigma_{BU} + \sigma_{(d,n)} + \sigma_{(d,p)} + \sigma_{(d,t)} + \sigma_{(d,\alpha)}}{\sigma_R} = 1 - \frac{\sigma_{DI}}{\sigma_R}. \quad (2)$$

The energy dependence of the above mentioned reduction factor is shown for deuteron interaction with ^{52}Cr, ^{56}Fe, ^{58}Ni, ^{93}Nb target nuclei at the top of Fig. 6 while at the bottom of the same figure the excitation functions of the DI and its components, BU, stripping and pick-up reactions are shown. Firstly, one may note a steep increases with energy of the reduction factor since the major BU but also and especially the DR components increase with energy. Most significant in this respect is the maximum of the (d, p) and (d, n) stripping excitation functions around 6-8 MeV, which provides the fastest slope of this factor. Finally, the reduction factor reaches its own maximum around deuteron energies of 15–20 MeV, and continues with a slow decrease due to the continuous increase of BU with the incident energy. The reduction factor values are close to around half of σ_R [3–5] at the deuteron incident energy of 50 MeV, pointing out the important DI role of the direct interactions.

5 Statistical particle emission

The statistical PE+CN reaction mechanisms which complete the deuteron interaction analysis along an enlarged nuclear-interaction time scale, become important with the increase of the incident energy above the Coulomb barrier. The corresponding reaction cross sections have been calculated using various versions of TALYS code [26], taking into account also the above-discussed BU, stripping, and pick–up results through the reduction factor of the optical model potential (OMP) total-reaction cross section. Another particular point of these calculations is the use of the same model parameters to account for different reaction mechanisms as, e.g., the same OMP parameters for calculation of the distorted waves in the ingoing/outgoing channels in direct reactions, of the PE transition rates, as well as of the transmission coefficients of various CN channels.

Additional PE+CN calculations have been carried out with the code STAPRE-H [27] for more detailed analysis involving particular options of various input parameters, e.g. for gamma-ray strength functions or initial p-h configurations.

The due consideration of all BU+DR+PE+CN is proved by the description of all measured data corresponding to deuteron interaction with a specific natural element target [2–5], e.g., activation excitation functions for d+^{nat}Ni interaction process shown in Fig. 2 [4].

The mark BU, rather than BF, for the sum of various contributions to an activation cross section in Figs. 1, 2, 4, and 5 underlines the consideration of both breakup effects, i.e., the overall decrease of σ_R, as well as the BF enhancement. On the other hand, the apparent discrepancies between the experimental data and corresponding TENDL-2017 [15] evaluation, shown in Figs. 1, 2, 4, and 5 stress out the effects of disregarding the direct processes within TENDL evaluation.

6 Conclusions

The present work has concerned a deeper analysis of the key role of DI, particularly of the breakup mechanism, in deuteron-induced reactions. The overall agreement between the measured data and model calculations supports the description of nuclear mechanisms taken into account for the deuteron-nucleus interaction, emphasizing the effects of direct interactions so far ignored in the evaluation procedures.

However, while the associated theoretical models for stripping, pick-up, PE and CN are already settled, an increased attention should be paid to the theoretical description of the breakup mechanism, including its inelastic component. The recently increased interest on the theoretical analysis of the breakup components [6, 7, 28, 29] may lead eventually to the refinement of the deuteron breakup empirical parametrization and increased accuracy of the deuteron activation cross section calculations, well beyond reaction cross sections recommended most recently for high-priority elements still using data fit by various-order Padé approximations [13].

On the other hand, the improvement of the deuteron breakup description requires, beyond the increase of its own data basis, also complementary measurements of (d, px) and (n, x), as well as (d, nx) and (p, x) reaction cross sections for the same target nucleus, within corresponding incident-energy ranges.

Acknowledgments

This work was partly supported by Autoritatea Nationala pentru Cercetare Stiintifica (Project PN-16420102), within the framework of the EUROfusion Consortium and has received funding from the Euratom research and training programme 2014-2018 under grant agreement No 633053. The views and opinions expressed herein do not necessarily reflect those of the European Commission.

References

[1] M. Avrigeanu and V. Avrigeanu, Phys. Rev. C **92** (2015) 021601(R).

[2] M. Avrigeanu, V. Avrigeanu, and A. J. Koning, *Phys. Rev.* C **85** (2012) 034603. M. Avrigeanu and V. avrigeanu, *Proceedings of the 14th International Conference on Nuclear Reaction Mechanisms Varenna, Italy, 2015*, edited by F. Cerutti *et al.*, CERN-Proceedings-2015-001 (CERN, Geneva, 2015), pp. 203 – 208; *J. Phys: Conf. Ser.* **724** (2016) 012003; *J. Phys: Conf. Ser.* **1023** (2018) 012009; M. Avrigeanu, V. Avrigeanu, and C. Costache *EPJ Web of Conferences* **146** (2017) 012020.

[3] P. Bém *et al.*, Phys. Rev. C **79** (2009) 044610; E. Šimečková *et al.*, Phys. Rev. C **84** (2011) 014605; M. Avrigeanu *et al.*, Phys. Rev. C **88** (2013) 014612; M. Avrigeanu and V. Avrigeanu, Nucl. Data Sheets **118** (2014) 301; M. Avrigeanu *et al.*, Phys. Rev. C **89** (2014) 044613.

[4] M. Avrigeanu *et al.*, Phys. Rev. C **94** (2016) 014606.

[5] E. Šimečková *et al.*, Phys. Rev. C **98** (2018) 034606.

[6] Yuen Sim Neoh, Kazuki Yoshida, Kosho Minomo, and Kazuyuki Ogata, Phys. Rev. C **94** (2016) 044619.

[7] B. V. Carlson, R. Capote, and M. Sin, Few-Body Syst. **57** (2016) 307.

[8] M. Avrigeanu *et al.*, Fusion Eng. Design **84** (2009) 418.

[9] M. Avrigeanu and V. Avrigeanu, Phys. Rev. C **95** (2017) 024607.

[10] http://www.iter.org/proj

[11] http://www.ifmif.org/b/

[12] http://pro.ganil-spiral2.eu/spiral2/instrumentation/nfs

[13] A. Hermanne *et al.*, Nucl. Data Sheets **148** (2018) 338.

[14] Experimental Nuclear Reaction Data (EXFOR), www-nds.iaea.or.at/exfor

[15] A. J. Koning and D. Rochman, 'TENDL-2017: TALYS-based evaluated nuclear data library', Dec. 30, 2017.

[16] M. G. Mustafa, T. Tamura, and T. Udagawa, Phys. Rev. C **35** (1987) 2077.

[17] J. Pampus *et al.*, Nucl. Phys. **A311** (1978) 141; J. R. Wu, C. C. Chang, and H. D. Holmgren, Phys. Rev. C **19** (1979) 370; N. Matsuoka *et al.*, Nucl. Phys. A**345** (1980) 1; J. Kleinfeller *et al.*,Nucl. Phys. A **370** (1981) 205.

[18] M. Avrigeanu and A. M. Moro, Phys. Rev. C **82** (2010) 037601.

[19] M. Kamimura *et al.*, Prog. Theor. Phys. **89**, Suppl. 1, (1986) 1; N. Austern *et al.*, Phys. Rep. **154** (1987) 125; A. Deltuva, A. M. Moro, E. Cravo, F. M. Nunes, and A. C. Fonseca, Phys. Rev. C **76** (2007 064602); K. Ogata and K. Yoshida, Phys. Rev. C **94** (2016) 051603(R).

[20] C. Kalbach Walker, "Deuteron Breakup and ^{21}Na Production", in *Triangle University Nuclear Laboratory Progress Report* **XLII (2002-2003)**; www.tunl.duke.edu/publications/tunlprogress/2003/.

[21] I. J. Thompson, Comput. Phys. Rep. **7** (1988) 167; v. FRES 2.9 (2011).

[22] I. Iseri, M. Yahiro, and M. Kamimura, Prog. Theor. Phys. Suppl. **89** (1986) 84.

[23] P. Guazzoni *et al.*,Phys. Rev. C **83** (2011) 044614.

[24] R. M. DelVecchio, Phys. Rev. C **7** (1973) 677.

[25] Evaluated Nuclear Structure Data File (ENSDF), http://www.nndc.bnl.gov/ensdf/

[26] A. J. Koning, S. Hilaire, and S. Goriely, v. TALYS-1.9, 2017, http://www.talys.eu

[27] M. Avrigeanu and V. Avrigeanu 1995 *IPNE Report* NP-86-1995, Bucharest, and Refs. therein; http://www.oecdnea.org/tools/abstract/detail/iaea0971/; M. Avrigeanu and V. Avrigeanu, Comp. Phys. Comm. **112** (1998) 191; A.Harangozo, I.Stetcu, M.Avrigeanu, and V.Avrigeanu, Phys. Rev. C **58** (1998) 295.

[28] Jin Lei and A. M. Moro, Phys. Rev. C **97** (2018) 011601; *ibid.* **92** (2015) 061602.

[29] G. Potel *et al.*, Eur. Phys. J. A. **53** (2017) 178.